Adsorption structure of pyrazine on Si(100): Density-functional calculations

Sung Chul Jung and Myung Ho Kang
Department of Physics, Pohang University of Science and Technology, Pohang 790-784, Korea
(Received 12 June 2009; revised manuscript received 14 September 2009; published 15 December 2009)

We have studied the adsorption structure of pyrazine ($C_4H_4N_2$) on the Si(100) surface by using density-functional theory calculations within a slab representation. We found that the adsorption energetics strongly depends on the $C_4H_4N_2$ coverage. At 0.25 monolayer (one monolayer is defined as one pyrazine molecule per Si dimer), two different molecular configurations are equally favored in energy: the end-on model where $C_4H_4N_2$ adsorbs on the down atom of a Si dimer and the cross-row model where $C_4H_4N_2$ connects two dimer rows. At 0.5 monolayer, the interactions between adsorbed molecules results in a far stabilized cross-row configuration in which molecules arrange in series along the row-perpendicular direction. This cross-row chain configuration is in good accordance with the images of a recent scanning tunneling microscopy experiment. When including the van der Waals interactions in our calculations, the cross-row structures were found to have larger energy gains, thus being more favored in energy than the end-on structures. The adsorption picture of the present slab-model calculations differs from previous cluster-model calculations, which questions the accuracy of the cluster representation of this adsorbed system.

DOI: 10.1103/PhysRevB.80.235312 PACS number(s): 68.43.Bc, 68.43.Fg, 68.43.Mn

I. INTRODUCTION

Adsorption of organic molecules on the Si(100) surface has attracted much interest because of possible applications in the areas of molecular electronics, biological recognition, and chemical sensors.[1,2] One interesting organic group is the aromatic molecules containing delocalized π electrons, which, upon adsorption on Si(100), generally undergo a disruption of π conjugation via the formation of strong C—Si bonds.[3] For example, benzene (C_6H_6) forms the so-called "butterfly" structure with two C—Si bonds on a single Si dimer or the "tight-bridge" structure with four C—Si bonds on two adjacent Si dimers and simultaneously loses the ring's aromaticity by the orbital rehybridization.[2–4] The reaction picture becomes more complicated for heteroaromatic molecules in which one or more of the atoms in the ring are of an element other than carbon.

Pyrazine ($C_4H_4N_2$) contains two N atoms at the opposite ends of the ring (see Fig. 1). The hexagonal ring of pyrazine maintains the circular π bonds but is slightly modified due to the presence of the substituted N atoms containing lone-pair electrons. This elemental inhomogeneity of pyrazine increases the number of possible configurations for molecular adsorption, and it has been an intriguing question what structure is formed upon adsorption on Si(100). In their density-functional theory (DFT) calculations, Lu *et al.*[5] suggested two possible adsorption configurations for $C_4H_4N_2$/Si(100): One is a C-mediated adsorption where two opposite C atoms of pyrazine are bonded to two Si atoms of a single dimer, and the other is a N-mediated adsorption where one N atom is bonded to a Si dimer atom [see the nitrogen end-on configuration in Fig. 2(a)]. They found that the C-mediated adsorption is more stable in energy but has a barrier of 0.23 eV for molecular adsorption while the less stable N-end-on adsorption is barrierless. It was thus speculated that, while the N-end-on configuration would be the primary adspecies at low temperatures, the primary adspecies at elevated temperatures would be the C-mediated configuration. Later, in their high-resolution electron-energy loss spectroscopy (HREELS) and x-ray photoelectron spectroscopy (XPS) study, Huang *et al.*[6] suggested a different adsorption model where $C_4H_4N_2$ adsorbs on top of a dimer [see Fig. 2(b)]. This on-top model was based on the evidence of two equivalent N—Si bonds and no C—Si bonds in the chemisorbed $C_4H_4N_2$ molecules at 300 K. Recently, in a combined scanning tunneling microscopy (STM), photoelectron diffraction (PED), and DFT study, Shimomura *et al.*[7] proposed the cross-row model where $C_4H_4N_2$ connects two dimer rows [see Fig. 2(d)]. This model explains well the room-temperature STM images indicating that $C_4H_4N_2$ molecules reside in between dimer rows and is also compatible with the earlier experimental data of Huang *et al.*[6] The combined DFT calculations, how-

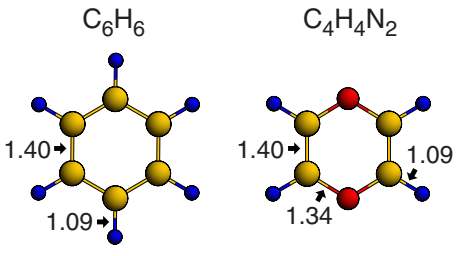

FIG. 1. (Color online) Structures of the C_6H_6 and $C_4H_4N_2$ molecules. The balls represent C, N, and H atoms with decreasing size. The calculated bond lengths are given in Å.

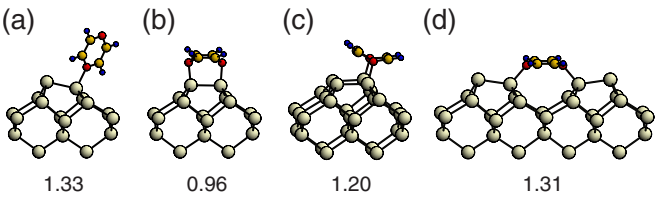

FIG. 2. (Color online) Optimized geometries of the 0.25 ML adsorption models for the $C_4H_4N_2$/Si(100) surface: (a) the end-on, (b) the on-top, (c) the end-bridge, and (d) the cross-row models. The adsorption energies are given in eV/molecule.

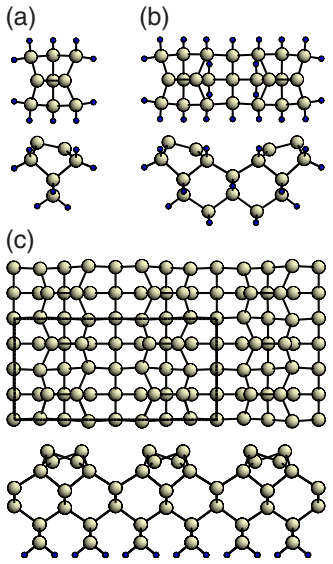

FIG. 3. (Color online) Schematic of the Si(100) surface models: (a) the previous Si_9H_{12} cluster (Ref. 5), (b) the previous $Si_{23}H_{24}$ cluster (Ref. 7), and (c) the present slab. Solid line represents the (4×2) unit cell.

ever, provided a conflicting result that the proposed cross-row model is far less stable by 0.54 eV than the end-on model. Thus, there remains a question why the more stable end-on model does not appear in the experimental studies. In connection with the question, we note that the previous DFT calculations used cluster models to represent the Si(100) surface.[5,7] As shown in Fig. 3, the employed cluster models consist of only a few Si atoms, many of which are terminated by H atoms. The validity of the use of such cluster models, however, has been in question in recent DFT studies for molecule adsorbed Si(111) surfaces. It was pointed out that the H terminations of subsurface Si atoms could make the Si atoms unphysically flexible and possibly affect the adsorption structure, energetics, and reaction mechanism.[8,9] Thus, in light of the conflict with the experimental observations, the previous cluster calculations[5,7] for the $C_4H_4N_2$/Si(100) surface may suffer the same problem of the overflexibility of H-terminated subsurface Si atoms.

In this work, we determine stable adsorption configurations of the $C_4H_4N_2$/Si(100) surface by carrying out DFT calculations with use of a slab representation of the surface. At a coverage of 0.25 monolayer (ML), we find that the end-on and cross-row models are the most stable structures. The cross-row model appears to be equally stable as the end-on model, contrary to the preference of the end-on model in the previous DFT-cluster study.[7] At a higher coverage of 0.5 ML, the interactions between adsorbed molecules result in a far stabilized cross-row configuration in which molecules arrange in series along the row-perpendicular direction. This cross-row chain configuration is shown to well explain the recently reported HREELS, XPS, and STM features.[6,7]

II. METHOD

We perform DFT calculations using the Vienna *ab initio* simulation package.[10] Exchange and correlation is treated by the generalized gradient approximation,[11] and ionic potentials are represented by ultrasoft pseudopotentials.[12] We expand the electronic wave functions in a plane-wave basis set of 25.6 Ry. The Si(100) surface is simulated by a periodic slab geometry with a (4×2) surface unit cell [see Fig. 3(c)]. Each slab consists of six atomic layers, and the vacuum spacing is about 12 Å. The bottom of the slab is passivated by two H atoms per Si atom. $C_4H_4N_2$ molecules are adsorbed on the top of the slab, where Si atoms are in the $c(4\times2)$ buckled-dimer configuration. The contact potential difference arising from the use of such asymmetric slab is corrected by using the correction scheme of Neugebauer and Scheffler.[13] Brillouin-zone integrations are done with a $2\times4\times1$ k-point mesh. The calculated bond length of the bulk Si is 2.364 Å. All atoms but the bottom two Si layers held at bulk positions are relaxed until the residual force components are within 0.1 eV/Å. The adsorption-energy differences calculated with the used parameters were found to converge within 0.01 eV as shown in Table I.

III. RESULTS

In this study, we consider two different pyrazine coverages, θ=0.25 ML and 0.5 ML. The coverage of 0.25 ML was chosen to represent an isolated $C_4H_4N_2$ molecule with a sufficiently large intermolecular separation. We found in our test calculations using a larger (4×4) surface unit cell that

TABLE I. Adsorption energies of $C_4H_4N_2$/Si(100) at a coverage of 0.25 ML. N_{layer}, k mesh, and E_{cut} represent the slab thickness of the Si substrate, the subdivisions of the (4×2) surface Brillouin zone, and the plane-wave cut-off energy, respectively. E_a and ΔE_a represent the adsorption energy and the adsorption-energy difference between the end-on and cross-row structures, respectively.

N_{layer}	k mesh	E_{cut} (Ry)	E_a (eV)		ΔE_a (eV)
			End-on	Cross-row	
6	$2\times4\times1$	25.6	1.331	1.307	0.024
8	$2\times4\times1$	25.6	1.342	1.310	0.032
6	$3\times6\times1$	25.6	1.333	1.309	0.024
6	$2\times4\times1$	31.9	1.334	1.307	0.027

TABLE II. Summary of the calculations for the $C_4H_4N_2/Si(100)$ surface. θ (ML) represents the $C_4H_4N_2$ coverage. E_a (eV) represents the adsorption energy. d (Å) represents the bond length between the given surface atoms. $\Delta z_{N—C}$ (Å) represents the molecular rumpling, defined as the vertical height of the N atoms from a plane containing the four C atoms. $d_{Si—Si}$ (Å) and $\Delta z_{Si—Si}$ (Å) represent the bond length and buckling in the $C_4H_4N_2$-adsorbed Si dimer, respectively.

Systems	θ	Models	E_a	$d_{N—C}$	$d_{C—C}$	$\Delta z_{N—C}$	$d_{N—Si}$	$d_{Si—Si}$	$\Delta z_{Si—Si}$
$C_4H_4N_2$				1.34	1.40	0			
Si(100)								2.36	0.73
$C_4H_4N_2/Si(100)$	0.25	End-on	1.33	1.34–1.36	1.38–1.39	0	1.89	2.43	0.51
		Cross-row	1.31	1.39	1.36	0.25	1.88	2.46	0.36
		End-bridge	1.20	1.43	1.34	0.39	1.80	2.41	0.05
		On-top	0.96	1.44	1.34	0.49	1.82	2.41	0
	0.5	End-on(S)	1.36	1.34–1.36	1.38–1.39	0	1.89	2.44	0.47
		End-on(Z)	1.32	1.34–1.36	1.38–1.39	0	1.89	2.43	0.50
		Cross-row(S)	1.56	1.42	1.34	0.28	1.80	2.56	0.06
		Cross-row(Z)	1.21	1.40	1.35	0.26	1.87	2.43	0.27

the calculated adsorption energies for the most stable structures little change (less than 0.02 eV per molecule) when we lower the coverage from 0.25 to 0.125 ML. The coverage of 0.5 ML was chosen to check the effect of intermolecular interactions at high coverages and also for comparison with experiments. In fact, previous experimental studies provided no quantitative information about the coverages, but we believe that the experimental coverages are close to 0.5 ML. In the HREELS and XPS study of Huang *et al.*[6] the coverage seems to be a near saturation because the data were obtained for the remaining chemisorbed molecules after annealing the multilayer pyrazine-covered sample to drive away all the physisorbed molecules, and we best estimate the local coverage of the high-coverage areas found in the STM images of Shimomura *et al.*[7] to be 0.5 ML [see Figs. 2(b) and 2(c) of Ref. 7].

A. Coverage of 0.25 ML

Figure 2 shows four structural models considered here: the end-on, on-top, end-bridge, and cross-row models. The end-on model with one N—Si bond was suggested in the DFT study of Lu *et al.*,[5] and the on-top and cross-row models with two N—Si bonds were suggested in the HREELS and XPS study of Huang *et al.*[6] and in the STM and PED study of Shimomura *et al.*,[7] respectively. As another possibility, we add the end-bridge model where $C_4H_4N_2$ connects the sides of two adjacent dimers in a row, forming two N—Si bonds [see Fig. 2(c)]. Here, we consider only the N—Si bonding configurations based on the experimental (HREELS and XPS) fact that the $C_4H_4N_2$ adsorption occurs exclusively through the N—Si bondings without involving C—Si bondings.[6] It was reported in the cluster calculations of Lu *et al.*[5] that there is an energy barrier of 0.23 eV for the C-mediated adsorption, and our slab calculations have also verified the presence of energy barriers of ~0.1 eV for the formation of C—Si bondings, while there is no energy barrier for N—Si bondings. Pyridine (C_5H_5N) with a chemical similarity to pyrazine is also known to initially react with Si(100) via a N—Si bonding, which is due to a favorable interaction between the lone-pair state of the N atom and the empty dangling-bond (DB) state of the down atom of a Si dimer.[14]

We find in our total-energy calculations that the end-on structure is the most stable with the adsorption energy 1.33 eV, which compares well with 1.17 and 1.21 eV for the similar N-end-on structures found in $C_5H_5N/Si(100)$ (Ref. 14) and $NH_3/Si(100)$,[15] respectively. It is also noticeable that the cross-row structure is almost equally stable with 1.31 eV. This finding provides a theoretical support for the experimental proposal of the cross-row structure by Shimomura *et al.*,[7] which was in conflict with their own DFT-cluster calculations that the cross-row model is far less stable by 0.54 eV than the competing end-on model. The end-bridge structure is less stable by 0.13 eV than the end-on structure. The on-top structure is the least stable with the adsorption energy 0.96 eV, which does not support the experimental suggestion of this model by Huang *et al.*[6]

The atomic structures shown in Fig. 2 represent the optimized geometries of the four structural models, and their structural details are summarized in Table II. In the end-on structure, $C_4H_4N_2$ forms a N—Si bond with the length 1.89 Å. The formation of the N—Si bond affects the structure of the underlying Si dimer. The dimer is elongated from 2.36 to 2.43 Å, and its buckling height is reduced from 0.73 to 0.51 Å. In contrast, the molecular structure is little changed. The changes in intramolecular bond lengths are all less than 0.02 Å, implying that the adsorbed molecule still maintains the ring's aromaticity. The adsorption energy of the end-on structure was found to strongly depend on the molecular orientation about the N—Si axis (see Fig. 4): At equilibrium, the angle between the dimer row and a surface-parallel line on the molecular plane is about 45°, and there is an energy barrier of 0.20 eV for the molecular rotation about the N—Si axis. In the study of Shimomura *et al.*,[7] the interaction between N and Si was regarded as a dative bonding in which the N atom donates the lone-pair electrons to the electron-deficient down Si atom. This intuitive chemical picture is supported by our calculations. We find that the calculated small adsorption energy, negligible molecular distor-

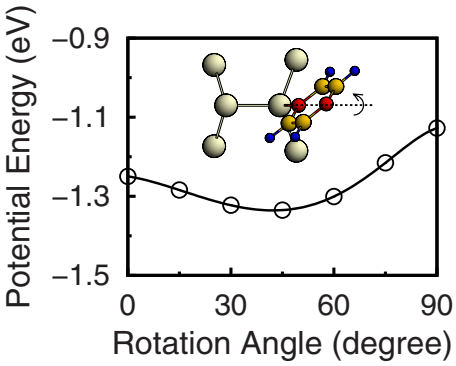

FIG. 4. (Color online) Energy diagram for the molecular rotation about the N—Si axis in the end-on model. The angle zero corresponds to a configuration with the molecular plane perpendicular to the dimer row.

tion, and partial recovery of the dimer buckling compare well with the adsorption properties of the NH_3/Si(100) surface, which is known to form a N—Si dative bonding.[15] The N—Si bond length 1.89 Å calculated for $C_4H_4N_2$ is somewhat smaller than 2.01 Å for NH_3,[15] but this difference is possibly attributed to the difference in electronic configuration of the N atom between $C_4H_4N_2$ and NH_3.

The other three models in Fig. 2 are all featured by two N—Si bonds. While the N—Si bond length in the cross-row model is 1.88 Å, comparable with 1.89 Å in the end-on model, the end-bridge and on-top models have shorter bonds of 1.80–1.82 Å. In addition, large molecular deformations of $C_4H_4N_2$ are a common feature of the three models. The two C—C bonds are contracted by 0.04–0.06 Å from 1.40 Å, the four N—C bonds are elongated by 0.05–0.10 Å from 1.34 Å, and there are rumplings of 0.25–0.49 Å in the molecular plane. The contraction of the C—C bonds and elongation of the N—C bonds is an indication of the disruption of π conjugation. The π electrons are rather localized than being evenly distributed over the entire ring. The π electrons of C participate in the C=C π bondings, and the π electron of N interacts with the bonded Si atom, forming a stronger covalent N—Si bonding, which is evident by the decreased N—Si distances and decreased dimer bucklings. Our calculations show that the bond strength increases in the order of cross-row, end-bridge, and on-top models. The molecular rumplings can be understood as an indication of large strain induced by the strong bondings at both N ends of the molecule. In view that these models have one more N—Si bond but are less stable than the end-on model, the energy gain related to the N—Si bond formation does not seem to compensate the loss of the resonance stabilization energy in the π-conjugated system.

Figure 5 shows the projected density of states (PDOS) of the end-on and cross-row adsorption configurations in comparison with those of the isolated pyrazine molecule and the clean Si(100) surface. In the end-on structure, only one N atom participates in the surface bonding. The N—Si dative bonding results in the extinction of the dangling-bond peak for the down-Si atom and the N contribution to the HOMO −1 peak. In the same time, the highest occupied molecular orbitals (HOMO, HOMO−1, and HOMO−2) and the lowest

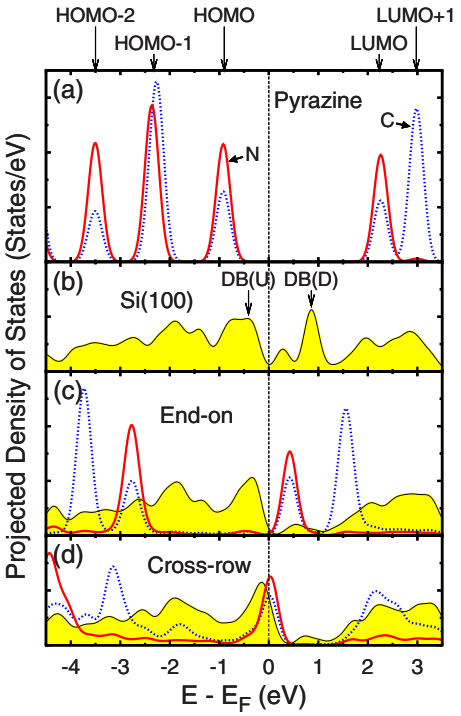

FIG. 5. (Color online) PDOS for the N and C atoms of the pyrazine molecule and the Si atoms of a surface dimer in different environments: (a) the isolated pyrazine molecule, (b) the clean Si(100) surface, (c) the end-on structure, and (d) the cross-row structure. Solid (dashed) lines represent the PDOS of the nitrogen (carbon) orbitals. In (a), HOMO and LUMO represent the highest occupied molecular orbital and the lowest unoccupied molecular orbital, respectively. In (b), DB(u) and DB(d) represent the dangling-bond states of the up-Si atom and the down-Si atom, respectively.

unoccupied molecular orbitals (LUMO and LUMO+1) shift almost rigidly toward lower energies by 1.4–1.8 eV with some peak broadening and weakening. These rigid, downward shifts of the molecular orbitals indicate that there is a potential drop from the vacuum level when the molecule approaches toward the surface[16] and the adsorbed pyrazine molecule still maintains its aromaticity. In the cross-row structure, the molecular orbitals undergo more significant changes than in the end-on case. The PDOS spectra related with the C atoms as well as the N atoms are noticeably deformed, reflecting the disruption of π conjugation due to the molecular rumpling. A relatively large upward shift ($\sim$0.2 eV) of the dangling-bond state of the up-Si atom also reflects its larger reduction in the dimer buckling.

Figure 6 shows the simulated STM images of the end-on and cross-row models. While the end-on model produces a rugged protrusion with its center on the down-atom side of the reacted dimer, the cross-row model produces a peanutlike protrusion between two dimer rows with the long axis along the dimer row. The much brighter image of the end-on model reflects the more protruding molecular structure. For microscopic examination of the adsorption structure, we should take into account a possibility of easy structural conversion between the two stable end-on and cross-row structures. We found that there is a straightforward conversion pathway, in

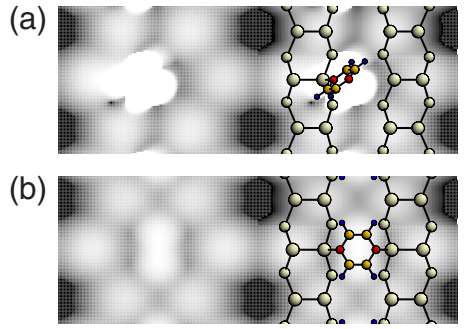

FIG. 6. (Color online) Simulated constant-current STM images of the 0.25 ML adsorption models: (a) the end-on and (b) the cross-row models. The images ware obtained by integrating $\rho(r,E)$ from $E_F-1.4$ eV to E_F and were taken at $\rho=5\times10^{-5}$ e/Å^3.

which the upright $C_4H_4N_2$ molecule in the end-on model lies down toward the adjacent row with its top N atom forming a new bond to the nearest Si atom in the row, and the corresponding energy barrier is 0.47 eV. The rate for the end-on to cross-row conversion and vice versa is estimated to be as fast as $\sim1.3\times10^6$ s^{-1} at 300 K by using an Arrhenius-type activation process with a typical value[17] ($\sim10^{14}$ Hz) for the pre-exponential factor. Thus, the present simulated images could be helpful in identifying low-coverage adsorption structures in future low-temperatures STM experiments.

We find that the present slab calculations differ from previous cluster calculations (see Table III). Particularly noticeable is the difference in the relative stability of the end-on and cross-row structures: while the cross-row model was calculated to be far less stable by 0.54 eV than the end-on model in the $Si_{23}H_{24}$ cluster calculations,[7] it appears to be equally stable with a negligible energy difference of 0.02 eV in the present slab calculations. It is interesting to consider the origin of such difference in energy between the present and previous theories. As was mentioned earlier, the Si atoms in the $Si_{23}H_{24}$ cluster model are mostly H terminated [see Fig. 3(b)]. This artificial H termination could increase the structural flexibility of the Si atoms and thus possibly lead to inaccurate molecule-surface reaction pictures.[8,9] Such indications are evident in the bond lengths reported in the $Si_{23}H_{24}$ cluster calculations.[7] In the cross-row structure, the N—Si and Si—Si bond lengths are shorter by 0.10 and 0.06 Å, respectively, than our slab calculations, implying that the Si atoms in the two $C_4H_4N_2$-adsorbed dimers displace toward the $C_4H_4N_2$ molecule. This movement of Si dimer atoms could cause a larger molecular distortion, resulting in a considerable loss of the resonance stabilization energy. The N—C and C—C bond lengths are longer by 0.04 Å and shorter by 0.02 Å, respectively, than our slab calculations. The end-on structure is also affected by the atomic flexibility, but in this case the effect is rather constructive. In the $Si_{23}H_{24}$ cluster, the end-on structure has one bare dimer, not occupied by $C_4H_4N_2$. If the Si atoms in this bare dimer displace toward the adsorbed $C_4H_4N_2$ molecule, an additional molecule-surface interaction occurs, thereby more stabilizing the end-on structure. This reasoning is supported by that the earlier calculations[5] using a Si_9H_{12} cluster with no bare dimer produced a smaller adsorption energy by 0.19 eV than the $Si_{23}H_{24}$ cluster calculations. Thus, a possibly underestimated (overestimated) adsorption energy for the cross-row (end-on) structure in the cluster calculations could lead to a large energy difference between the two, otherwise equally stable, structural models.

B. Coverage of 0.5 ML

We considered several $C_4H_4N_2$ configurations possible at 0.5 ML using the stable end-on and cross-row models as basic building units. Figure 7 shows four representative stable configurations. Figure 7(a) shows the end-on(S) configuration in which $C_4H_4N_2$ molecules are in a square arrangement with the adsorption energy 1.36 eV. Here, all the molecules have the equilibrium angle of 45° with respect to the perpendicular direction to the dimer row. An alternation of the equilibrium angles of 45° and −45° is also equally stable with the adsorption-energy difference within 0.01 eV. Figure 7(b) shows the end-on(Z) configuration with a zigzag arrangement of molecules, which is less stable by 0.04 eV than the end-on(S) configuration. We notice that the adsorption energies of the two end-on configurations at 0.5 ML are comparable with that of the end-on structure at 0.25 ML, implying that the interaction between adjacent end-on pyrazines is not strong even at 0.5 ML. Figure 7(c) shows the cross-row(S) configuration with a square arrangement of molecules. This configuration is characterized by a dimer-mediated successive connection between molecules along the direction perpendicular to the row and has a large adsorption energy of 1.56 eV. On the other hand, the cross-row(Z) configuration with a zigzag arrangement, shown in Fig. 7(d),

TABLE III. Calculation results in the present slab and previous cluster studies for the $C_4H_4N_2$/Si(100) surface. E_a, $d_{N—Si}$, $d_{Si—Si}$, $d_{N—C}$, and $d_{C—C}$ are defined in Table II. The cluster sizes used in previous studies are given in the parentheses.

	End-on			Cross-row				
Methods	E_a	$d_{N—Si}$	$d_{Si—Si}$	E_a	$d_{N—Si}$	$d_{N—C}$	$d_{C—C}$	$d_{Si—Si}$
Present slab	1.33	1.89	2.43	1.31	1.88	1.39	1.36	2.46
Cluster[a] ($Si_{23}H_{24}$)	1.00	1.97	2.39	0.46	1.78	1.43	1.34	2.40
Cluster[b] (Si_9H_{12})	0.81	1.99	2.37					

[a]Reference 7.
[b]Reference 5.

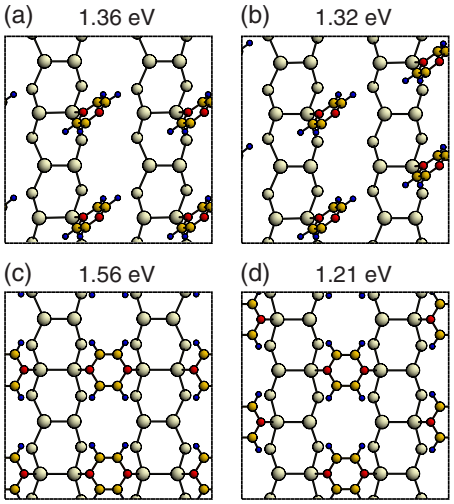

FIG. 7. (Color online) Optimized geometries of the 0.5 ML adsorption models for the $C_4H_4N_2/Si(100)$ surface: (a) the end-on(S), (b) the end-on(Z), (c) the cross-row(S), and (d) the cross-row(Z) models. The adsorption energies are given in eV/molecule.

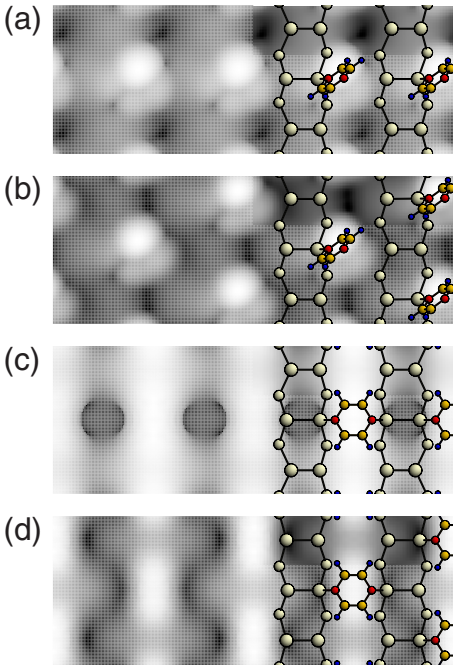

FIG. 8. (Color online) Simulated constant-current STM images of the 0.5 ML adsorption models: (a) the end-on(S), (b) the end-on(Z), (c) the cross-row(S), and (d) the cross-row(Z) models. The image were obtained by integrating $\rho(r,E)$ from $E_F-1.4$ eV to E_F and were taken at $\rho=5\times10^{-6}$ e/Å^3.

is much less stable by 0.35 eV than the cross-row(S) configuration, indicating that the energetics of the cross-row configurations is sensitive to the molecular arrangement. A noticeable structural difference between the cross-row(Z) and cross-row(S) configurations is the number of Si dangling bonds. While the former leaves a half-filled dangling bond in the reacted Si dimer, the latter saturates all dangling bonds of the reacted dimer. The large energy gain of 0.35 eV can be attributed to this elimination of half-filled Si dangling bonds.

Table II summarizes the structural details of the four configurations shown in Fig. 7. The end-on(S) and end-on(Z) configurations are similar in substrate atomic structure to the 0.25 ML end-on structure. The local structure of the cross-row(Z) configuration is also similar to the 0.25 ML cross-row structure, except a little reduced Si dimer buckling from 0.36 to 0.27 Å. On the other hand, the most stable cross-row(S) configuration reveals noticeable changes in local bonding configuration compared to the 0.25 ML cross-row structure: The N—Si bond length decreases from 1.88 to 1.80 Å, the Si—Si bond increases from 2.46 to 2.56 Å, and the buckling height decreases from 0.36 to 0.06 Å, indicating that the saturation of the activated dangling bond of the reacted dimer makes the Si—Si dimer more symmetric and eases a stronger N—Si bond formation.

Figure 8 shows the simulated STM images of the four 0.5 ML configurations. Similar to the 0.25 ML cases, the end-on configurations show bright dots with subsidiary protrusions around the down-atom side of the reacted dimers, and the cross-row configurations rectanglelike protrusions between two dimer rows. Unlike the 0.25 ML cases, the images of Si dimer atoms are not clearly seen in all 0.5 ML configurations. In their room-temperature STM study, Shimomura *et al.*[7] observed elliptical protrusions corresponding to the $C_4H_4N_2$ adsorbates with the center located at the halfway between the dimer rows and on the line connecting the dimer bonds. Moreover, it was found that the elliptical protrusions tend to linearly align along the row-perpendicular direction [see Fig. 2(c) of Ref. 7]. This STM feature was assigned to the formation of a linear chain configuration of cross-row adsorptions, the physical origin of which was suggested as a way of reducing the number of the Si dangling bonds activated by single cross-row adsorptions.[7] In fact, we find that the simulated image of the cross-row(S) configuration [see Fig. 8(c)] well reproduces the STM feature of linear images, which constitutes a microscopic confirmation of the energetically favorable cross-row chain configuration.

The adsorption structure in the cross-row(S) configuration well accounts for the HREELS and XPS results of Huang *et al.*[6] The presence of two equivalent N—Si bonds is compatible with the HREELS feature associated with the N—Si stretching mode and the XPS spectra indicating the chemically indistinguishable two N atoms. Moreover, the C—C bond contraction by 0.06 Å from 1.40 Å is in agreement with the HREELS observation of a vibrational peak attributed to the nonconjugated C=C double bond. The disruption of π conjugation discussed already at 0.25 ML is also consistent with the HREELS report that the characteristic vibrational modes of aromatic ring are absent in the spectra.

IV. DISCUSSIONS

In the course of our study, we came across a notion that van der Waals (vdW) interactions may be important not only in weakly interacting systems but also in chemically bonding systems, as well illustrated in a recent DFT study of Johnston *et al.*[18] for the benzene (C_6H_6) on the Si(100) surface. It was found that, when including a correction using the vdW-DF developed by Dion *et al.*,[19] the butterfly structure becomes

TABLE IV. Adsorption energies (eV) for the end-on and cross-row configurations before and after the vdW corrections.

	0.25 (ML)		0.5 (ML)	
Methods	End-on	Cross-row	End-on(S)	Cross-row(S)
DFT	1.33	1.31	1.36	1.56
DFT+vdW	1.84	1.98	1.87	2.26

more stable than the tight-bridge structure, the previously most stable in several DFT studies without vdW corrections. It is thus interesting to examine the influence of the vdW interaction on the present $C_4H_4N_2/Si(100)$ system. For this purpose we estimated the vdW corrections to the pyrazine adsorption energies by employing the vdW-DF(PBE) code developed by Lazić *et al.*,[20] which effectively evaluates the vdW energy as a postprocessing procedure starting from the electron density of the equilibrium adsorption structures obtained from our DFT calculations without vdW corrections.

Table IV shows the adsorption energies for the end-on and cross-row configurations before and after the vdW corrections. At 0.25 ML, the vdW interaction results in large increases in adsorption energy, which amount to 0.51–0.67 eV, much larger than the increases of 0.02–0.25 eV reported for the $C_6H_6/Si(100)$ surface.[18] Especially, the cross-row structure has a more energy gain by the vdW interaction and, as a result, becomes more stable by 0.14 eV than the competing end-on structure. The more energy gain in the cross-row structure can be attributed to its flat-lying configuration. In that geometry, the atoms of the pyrazine are much closer to the surface than in the upright end-on configuration, possibly resulting in a larger vdW interaction. At 0.5 ML, the vdW corrections in adsorption energy are 0.51–0.70 eV, almost the same as at 0.25 ML. This result implies that the vdW contribution is mostly from the molecule-surface interactions, like the case of the $C_6H_6/Si(100)$ surface.[18] In summary, the present perturbative incorporation of the vdW interaction turns out to reinforce the status of the cross-row structure as the most energetically favored configuration even at low coverages. In view of the relatively large vdW corrections, however, a correct determination of the adsorption energetics in this system may require a fully self-consistent estimation of the vdW energy and forces and the resulting structural relaxations, which will be done later with the use of more developed vdW-DF functionals and codes.

V. SUMMARY

We have studied the adsorption structure of $C_4H_4N_2$ on the Si(100) surface by using DFT-slab calculations. We found that at 0.25 ML the end-on and cross-row structures are equally stable in energy, but, at 0.5 ML, the interactions between adsorbed molecules result in a far stable, cross-row chain configuration in which molecules arrange in series along the row-perpendicular direction. This result leads to an adsorption picture that an isolated $C_4H_4N_2$ molecule could form either end-on or cross-row structure with equal preference, but, at high coverages, the cross-row structures dominate with a tendency to form linear-chain configurations along the row-perpendicular direction. The calculated energetics, atomic structures, and microscopic images provide a unified theoretical explanation for the observed HREELS, XPS, and STM features. Our vdW-DF calculations support the idea that the van der Waals interaction is important and thus should be properly taken into account for theoretical studies of the adsorption energetics for covalently bonding systems.

ACKNOWLEDGMENTS

This work was supported by the Korea Research Foundation Grant funded by the Korea Government (Grant No. 2009-0074825).

[1] S. F. Bent, Surf. Sci. **500**, 879 (2002).
[2] M. A. Filler and S. F. Bent, Prog. Surf. Sci. **73**, 1 (2003).
[3] L. Fang, J. Liu, S. Coulter, X. Cao, M. P. Schwartz, C. Hacker, and R. J. Hamers, Surf. Sci. **514**, 362 (2002).
[4] J.-Y. Lee and J.-H. Cho, Phys. Rev. B **72**, 235317 (2005).
[5] X. Lu, X. Xu, J. Wu, N. Wang, and Q. Zhang, New J. Chem. **26**, 160 (2002).
[6] H. G. Huang, J. Y. Huang, Y. S. Ning, and G. Q. Xu, J. Chem. Phys. **121**, 4820 (2004).
[7] M. Shimomura, D. Ichikawa, Y. Fukuda, T. Abukawa, T. Aoyama, and S. Kono, Phys. Rev. B **72**, 033303 (2005).
[8] M. H. Kang, Phys. Rev. B **68**, 205307 (2003).
[9] S. C. Jung and M. H. Kang, J. Korean Phys. Soc. **51**, 130 (2007).
[10] G. Kresse and J. Furthmüller, Phys. Rev. B **54**, 11169 (1996).
[11] J. P. Perdew, in *Electronic Structure of Solids '91*, edited by P. Ziesche and H. Eschrig (Akademie, Berlin, 1991).
[12] D. Vanderbilt, Phys. Rev. B **41**, 7892 (1990).
[13] J. Neugebauer and M. Scheffler, Phys. Rev. B **46**, 16067 (1992).
[14] H.-J. Kim and J.-H. Cho, J. Chem. Phys. **120**, 8222 (2004).
[15] S. H. Lee and M. H. Kang, Phys. Rev. B **58**, 4903 (1998).
[16] S. Hong and H. Kim, J. Korean Phys. Soc. **49**, 2362 (2006).
[17] R. I. Masel, *Principles of Adsorption and Reaction on Solid Surfaces* (Wiley, New York, 1996), p. 607.
[18] K. Johnston, J. Kleis, B. I. Lundqvist, and R. M. Nieminen, Phys. Rev. B **77**, 121404(R) (2008).
[19] M. Dion, H. Rydberg, E. Schröder, D. C. Langreth, and B. I. Lundqvist, Phys. Rev. Lett. **92**, 246401 (2004).
[20] P. Lazić, N. Atodiresei, M. Alaei, V. Caciuc, S. Blügel, and R. Brako, arXiv:0810.2273 (unpublished).